THE JOURNAL OF PHYSICAL CHEMISTRY C
A JOURNAL OF THE AMERICAN CHEMICAL SOCIETY

pubs.acs.org/JPCC

Article

# Computational Study on the Lifting of Aluminum Particles from a Hydroxyl-Terminated Polybutadiene Burning Surface

Yuxin Zhou and Michael R Zachariah*

Cite This: J. Phys. Chem. C 2025, 129, 5696−5701

Read Online

ACCESS | Metrics & More | Article Recommendations

**ABSTRACT:** The addition of aluminum particulates to polymer fuels is desired as a means to increase energy density. While nanosized aluminum has some attractive features with respect to its micrometer counterpart in terms of the burn rate, when incorporated into a fuel such as hydroxyl-terminated polybutadiene (HTPB), its release is often retarded, leading to crust formation on the fuel grain surface. Here, we undertake a molecular dynamics study to understand the size dependence of the polymer−particle interaction and how this impacts the size dependence of particle ejection. Comparing the interaction energy with the kinetic energy imparted to particles from the lifting force during polymer pyrolysis, we find that indeed, nanosized aluminum, due to its increased particle−polymer interaction binding energy, does not eject from the surface, while micrometer aluminum will. This is consistent with the experimental observation in a stagnation-flow burner. Further theoretical analysis indicated that replacing Al nanoparticles by nanosized Al/nitrocellulose (NC) mesoparticles may enhance the lifting of particles since the gas expansion from NC decomposition can generate sufficient kinetic energy to overcome the binding energy with the polymer.

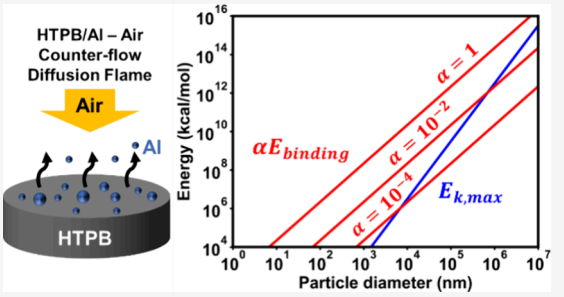




## 1. INTRODUCTION

The energy densities of metal and metalloid particles, for example, aluminum (Al, ∼84 kJ/cm$^3$), titanium (Ti, ∼89 kJ/cm$^3$), boron (B, ∼138 kJ/cm$^3$), and magnesium (Mg, ∼43 kJ/cm$^3$),[1−3] are generally higher than those of conventional hydrocarbon fuels such as diesel (∼35 kJ/cm$^3$),[4] liquid natural gas (∼22 kJ/cm$^3$),[4] and hydroxyl-terminated polybutadiene (HTPB, ∼34 kJ/cm$^3$),[5] which is a widely used de facto polymer fuel.[6,7] Thus, premixing metal/metalloid particles with a polymeric fuel has long been considered a strategy to increase the energy density for air-breathing propulsion.

However, the development of air-breathing metal-loaded solid fuels is inherently complicated since it involves multiple subprocesses including chemistry, multiphase fluid mechanics, and heat/mass transfer in multiple scales. To address the complexity, a stagnation-flow diffusion flame configuration as shown in Figure 1a provides a quasi-one-dimensional flame structure and relatively clear boundary conditions and has often been employed in fundamental combustion mechanism studies.[8−12]

Using this stagnation flow with HTPB, we can add varying amounts of the Al particles of different sizes. The basic experimental result for regression rates under conditions of a counterflow air velocity of 2.9 m/s and an air preheat temperature of 750 K is presented in Figure 1b. The fuel consumption rate increases slightly (roughly 10%) upon doping with 10 wt % microscale Al ($\mu$Al), which is also true for several different average-sized $\mu$Al. However, HTPB doped with 10 wt % nanoscale Al (nAl) fails to sustain a steady flame. Upon microscopic inspection, we observe an Al/$Al_2O_3$ crust on the top of the fuel grain. A similar phenomenon was also reported by Young et al.,[13] with added nAl, and showed

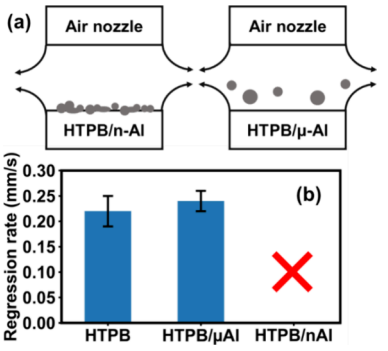


**Figure 1.** (a) Stagnation-flow burner configuration and the differences between the behavior of $\mu$Al and nAl on the surface of HTPB; (b) regression rates of HTPB, HTPB/$\mu$Al, and HTPB/nAl.

**Received:** December 17, 2024
**Revised:** February 18, 2025
**Accepted:** February 24, 2025
**Published:** March 6, 2025

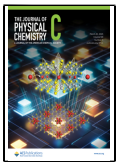




https://doi.org/10.1021/acs.jpcc.4c08542
J. Phys. Chem. C 2025, 129, 5696−5701

retardation of the regression rate of HTPB in a counterflow diffusion flame. This is despite the fact that nAl is known to be more reactive than $\mu$Al in a powder form. HTPB should pyrolyze to low-molecular-weight products that volatilize to the vapor phase, generating an upward fuel stream and forming a counterflow diffusion flame, with the downflowing air. The mole fraction of fuel is presumably near unity at the surface of HTPB, meaning that the surface is effectively in an anaerobic environment, with the possible exception of $H_2O$ and $CO_2$ back diffusion. Consequently, it is the vapor generation from fuel pyrolysis that lifts particles from the fuel grain, where they will eventually encounter oxygen and burn.

The basic motivation of the work is to explore the lifting process to elucidate the size effect on lifting observed experimentally, as shown in Figure 1.

In this study, we employ molecular dynamics (MD) simulation to assess the interaction energetics between particles and the surrounding polymer from which we assess how much energy is needed to lift the particle from the HTPB surface. This is compared to the kinetic energy imparted from the lifting force, leading to a scaling law that shows why $\mu$Al is lifted, while nAl is not. We further consider another strategy of using a mesoparticle containing a gas generator as a means to add an additional impetus to lift Al nanoparticles off the surface.

## 2. MD SIMULATION METHODS

The lifting of Al particles from the HTPB surface can be simplified as the competition between the HTPB surface−Al particle binding energy and the kinetic energy of an Al particle due to the blowing force from the fuel decomposition/volatilization to create lift.

Given the chemical complexity of HTPB, a simplified HTPB molecular structure is adopted from previous studies.[14,15] This simplified model comprises one *cis*-1,3-butadiene groups, one vinyl-1,2-butadiene group, three *trans*-1,3-butadiene group, and two terminal hydroxyl groups, as shown in Figure 2. The

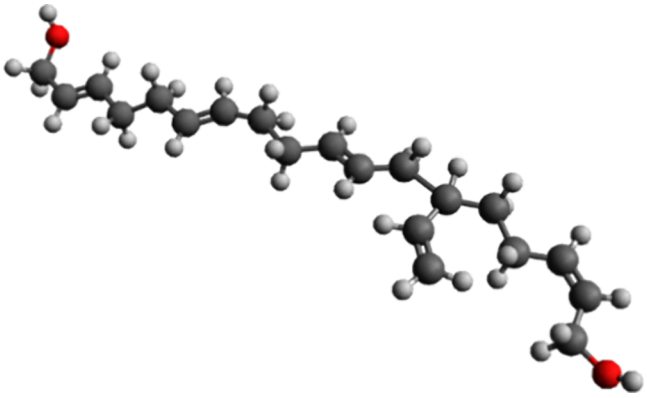

**Figure 2.** Structure of the simplified HTPB molecule ($C_{20}H_{32}O_2$). Gray, white, and red spheres represent C, H, and O atoms, respectively.

HTPB molecules are energy-minimized, relaxed at 400 K, and subsequently arranged at the base of the simulation domain with an initial density of approximately 0.65 g/cm$^3$, hereafter termed the "HTPB pool".

Al particles are typically covered by a native oxide shell; therefore, Al-core-$Al_2O_3$-shell nanoparticles are constructed in this study, following the detailed methodology described in our previous work.[16] Three Al-core-$Al_2O_3$-shell nanoparticles with different particle diameters (2.4, 4, and 6 nm) but similar shell thicknesses (roughly 0.8 nm) are created to investigate the dependency of the HTPB surface−Al particle binding energy on the particle size. They are composed of 671, 2759, and 8838 atoms, respectively. The internal core−shell structures of these Al nanoparticles are shown in Figure 3. All three nanoparticles are energy-minimized and relaxed at 400 K.

To simulate the interaction between the HTPB liquid and Al nanoparticles, a cavity is preformed during the construction of the HTPB pool. The Al nanoparticles are then positioned at various locations relative to the HTPB pool surface: above the surface, resting on the surface, and partially and fully immersed within the pool. The simulation domain sizes are 60 Å × 60 Å × 160 Å, 70 Å × 70 Å × 160 Å, and 90 Å × 90 Å × 160 Å, for 2.4, 4, and 6 nm particles, respectively. Periodic boundary conditions are applied in three dimensions. The centers of mass of particles are all located at the central vertical axis of the simulation domain. The entire system is subsequently energy-minimized and relaxed at 400 K for 2 ps. Figure 4 shows snapshots of the HTPB pool and a 4 nm Al particle after relaxation. The interaction energy $E_{\text{interaction}}$ between Al particles and HTPB can be calculated by

$$E_{\text{interaction}} = E_{\text{p,total}} - E_{\text{p,HTPB}} - E_{\text{p,Al}} \quad ((1))$$

$E_{\text{p,total}}$, $E_{\text{p,HTPB}}$, and $E_{\text{p,Al}}$ are the potential energy of the total system, HTPB pool, and Al particle, respectively.

The force field used in this work is Al/C/H/O ReaxFF developed by Hong and van Duin,[17] which has been employed in numerous similar scenarios such as the study on the interaction between Al nanoparticles and carbon fiber,[16] the carbon coating on the surface of Al nanoparticles,[17] Al/*n*-butanol nanofluid combustion,[18] and aluminum hydride/HTPB solid fuel combustion.[15] MD simulations in this work are performed in large-scale atomic/molecular massively parallel simulator (LAMMPS) software[19] with a time step of 0.2 fs. A Nose−Hoover thermostat[20] was used for temperature control with a damping parameter of 20 fs.

## 3. COMPUTATIONAL RESULTS AND DISCUSSION

**3.1. Analysis on Al-HTPB Binding Energy vs the Kinetic Energy of Al.** Figure 5a shows the evolution of the interaction energy between a 4 nm Al particle and HTPB liquid as the particle gradually sinks into the HTPB liquid. The interaction energy values are negative, indicating a stable interface. As the particle gradually sinks, the interaction energy increases. We define the binding potential energy $E_{\text{binding}}$ as the change in the interaction energy before and after the full submergence of particles into HTPB. We can assume that $E_{\text{binding}}$ should be proportional to the surface area of interaction, i.e., the particle surface area as shown in eq (2). Applying a linear fit to $k$, we can estimate the relationship between $E_{\text{binding}}$ and particle diameter $d$ based on the interaction energy for the three particle sizes computed. The fitting results are presented in Figure 5b.

$$E_{\text{binding}} = kd^2 \quad ((2))$$

It should be noted that the binding energy fitted in eq (2) is for the case of a fully submerged particle. Under partial submersion, we define $\alpha$ as the ratio of the interacting surface area to the total surface area. For example, $\alpha$ = 1 means that the particle is fully submerged, while $\alpha$ = 0.01 means that the



https://doi.org/10.1021/acs.jpcc.4c08542
J. Phys. Chem. C 2025, 129, 5696−5701

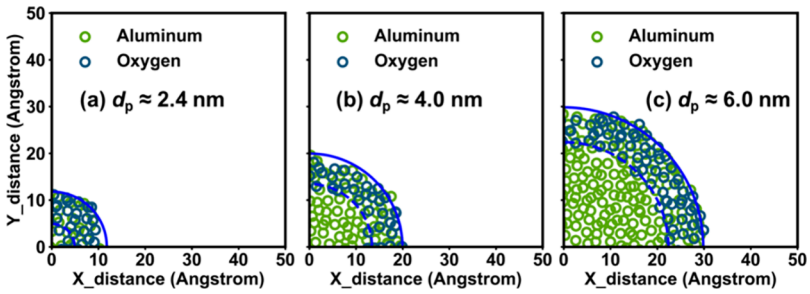


**Figure 3.** Sliced view of the Al nanoparticles of different particle diameters. Al and O atoms are shown in green and dark blue, respectively. The diameters of the particle and the Al core are shown in blue solid and dashed lines, respectively.

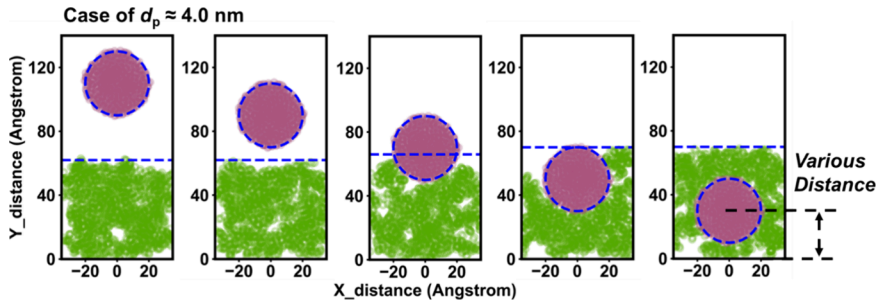


**Figure 4.** Snapshots of the HTPB pool and a 4 nm Al particle after relaxation. Al and C atoms are shown in pink and green symbols, respectively. H and O atoms are not presented in this figure for the sake of simplicity purposes. The outline of the Al particle and the surface of the HTPB pool are highlighted by blue dashed lines.

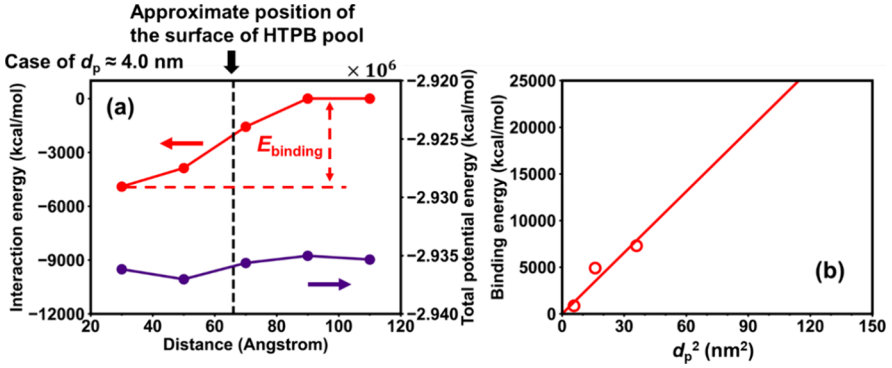


**Figure 5.** (a) Interaction energy between the HTPB pool and a 4 nm Al particle and the total potential energy as a function of the submersion depth. (b) Binding energy proportional to the particle surface area. Symbols are MD-calculated results, and the solid line is a linear fit.

particle is just sitting on the surface. The binding energy for the particle not fully submerged can be corrected by $\alpha$.

$$\alpha E_{\text{binding}} = \alpha k d^2 \quad ((3))$$

Following the determination of the binding energy between the Al particle and the HTPB, we are now in a position to estimate the likelihood of particle lift from the surface. To achieve the ejection of the particle from the surface, a particle must obtain a kinetic energy in excess of the binding energy.

This kinetic energy will come from the blowing force generated by the decomposition of HTPB, releasing gas-phase hydrocarbon species, such as $C_4H_6$.[8] The actual dynamics at the interface are complex, but we can assume that the drag force exerted by the upward gas flow is the sole force responsible for lifting the particle. It is important to note that thermophoresis is unlikely to assist in the lifting process as the surface of HTPB is cooler than the gas above, which would result in a net force acting against the lifting. Additionally, the influence of gravity can be considered to be negligible in this context. Consequently, we can infer that the maximum kinetic energy achievable by the particle due to the upward gas flow occurs when the velocity of the particle is relaxed compared to that of the upward gas flow.

Given that we have measured the regression rate $r$ of HTPB, as shown in Figure 1b, we can employ a mass flux balance to readily calculate the gas velocity of the pyrolysis products, by eq (4). Subsequently, this allows us to determine the maximum kinetic energy that the particle with a diameter of $d$ can acquire from eq (5).

$$v_{\text{particle}} = v_{\text{flow}} = \frac{\rho_{\text{HTPB}}}{\rho_{\text{gas}}} r \quad ((4))$$

$$E_{\text{k,max}} = \frac{1}{2} m v_{\text{particle}}^2 = \frac{1}{2} m v_{\text{flow}}^2 = \frac{1}{12} \pi \rho_{\text{Al}} d^3 v_{\text{flow}}^2 \quad ((5))$$

We now compare these two critical energies: the binding energy between the Al particle and the HTPB liquid, which



https://doi.org/10.1021/acs.jpcc.4c08542
J. Phys. Chem. C 2025, 129, 5696−5701

prevents its lifting, and the maximum kinetic energy of the Al particle, which facilitates lifting.

Figure 6 presents these two energies as a function of the particle diameter. The results are plotted as two sets of curves:

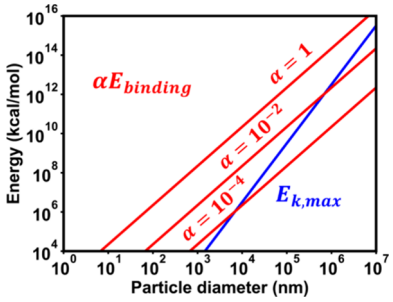


**Figure 6.** Dependency of $\alpha E_{binding}$ and $E_{k,max}$ on the particle diameter. Crossing points are the cutoff sizes at which smaller particles are held in the liquid and do not lift off.

the calculated binding energy (red, $\alpha E_{binding}$) and the maximum kinetic energy (blue, $E_{k,max}$), both with positive but different slopes. This occurs because the binding energy has a squared dependence on the diameter (eq (3)), while the maximum kinetic energy has a cubic dependence on the diameter (eq (5)).

Since $\alpha E_{binding}$ and $E_{k,max}$ have different slopes, these curves cross. The deeper the particles are embedded (larger $\alpha$), the more the kinetic energy is required, leading to crossing points at larger diameters. Particles larger than the crossing point have kinetic energies greater than the binding energy, and one should expect the particle to lift off the surface. This primarily occurs for particles nominally > ~10 $\mu$m. For smaller particles, however, the large surface-to-volume ratio results in a higher surface interaction with liquid HTPB and insufficient lifting force. This is consistent with our experimental observation that Al nanoparticles do not emerge from the HTPB surface and sinter to form a passivating crust. This analysis provides insight into why microsized Al particles can be ejected, whereas nanosized Al particles cannot, as observed in our experiments.

**3.2. Potential Strategy to Promote the Lifting of Al Nanoparticles.** Given the poor combustion characteristics of Al nanoparticles in HTPB experimentally and the above explanation, we propose a potential strategy to mitigate the accumulation of Al on the HTPB surface and promote particle lifting. Essentially, we need an additional source of kinetic energy. The idea comes from mesoparticles that are spherical aggregates of nanoparticles, generated by spray drying.[21] These aggregated spheres (typically 1−20 $\mu$m) composed of nano-Al, which are held together by a gas-generating binder such as nitrocellulose (NC).[21−24] The key unique feature of these materials is the low-temperature decomposition of the NC (as gas generator), which provides a propulsive force to deaggregate the particles with high velocity.

The concept then is whether such an Al/NC mesoparticle can generate sufficient kinetic energy to overcome the binding energy. When NC decomposes, it generates a mixture of gas-phase species (NO, $NO_2$, CO, $CO_2$, etc.),[25] which would result in a volumetric expansion of ~$10^3$ times, at 1 atm. Figure 7a shows a representation of the disassembly of Al/NC mesoparticles, while Figure 7b shows an experimental observation on the disassembly of Al/NC mesoparticles by high-speed microscopic imaging techniques, which has been discussed in detail in our previous study.[26]

Keeping in mind that the Al/NC mesoparticle is an assembly of Al nanoparticles in an NC matrix, it is reasonable to assume that the kinetics of NC decomposition will be much faster than the mechanical response of the nanoparticles. We assume that NC decomposition is effectively instantaneous, resulting in a thousand-fold increase in pressure. This assumption is based on the idealized conditions that no gas escapes and Al nanoparticles remain stationary and, as such, provides only an upper-limit estimation for the pressure inside the mesoparticles.

With this assumption and knowing that the NC content is typically ~10%, we can assume that the pressure, $P$, inside the mesoparticle just after the thermal decomposition of NC is ~100 atm (~$10^7$ Pa).

The high pressure generated by the thermal decomposition of NC exerts a force normal to the surface of the particle on the surrounding HTPB as illustrated in Figure 8. The idea is that this force can lift the particle. The spherical nAl/NC mesoparticle of radius $R$ can be expressed by eq (6).

$$x^2 + y^2 + z^2 = R^2 \qquad ((6))$$

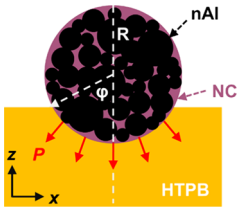


**Figure 8.** Diagram of an nAl/NC mesoparticle and forces on the surface of HTPB, during explosion.

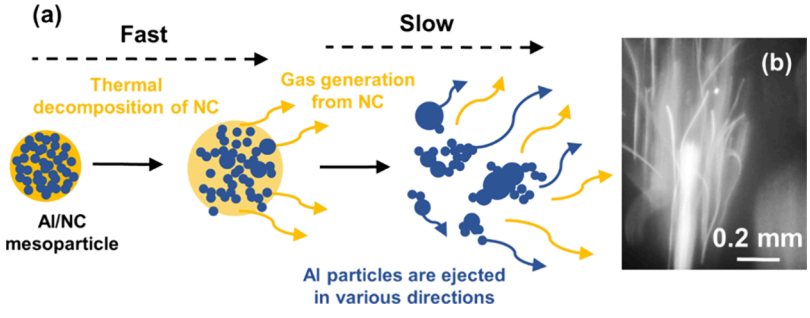


**Figure 7.** (a) Schematic diagram of the exploding of an Al/NC mesoparticle. (b) High-speed imaging of the exploding Al/NC mesoparticle.



https://doi.org/10.1021/acs.jpcc.4c08542
J. Phys. Chem. C 2025, 129, 5696−5701

When the angle between the vertical axis of particles and the HTPB interface is $\varphi$, the maximum possible resultant force, $F_z$, exerted by the HTPB on the particle can be presented by

$$\begin{aligned} F_z &= P\int \frac{z}{R}\mathrm{d}S \\ &= P\int \frac{\sqrt{R^2 - x^2 - y^2}}{R}\mathrm{d}S \\ &= P\int \frac{\sqrt{R^2 - x^2 - y^2}}{R}\sqrt{1 + \left(\frac{\partial z}{\partial x}\right)^2 + \left(\frac{\partial z}{\partial y}\right)^2}\,\mathrm{d}x\mathrm{d}y \\ &= P\pi R^2 \sin^2\varphi \end{aligned} \tag{7}$$

In eq (7), d$S$ is the differential area. Under the action of the aforementioned maximum possible resultant force $F_z$, if we define $\theta$ as the angle between the vertical axis of the particle and the HTPB interface as an integral variable ($\theta$: $\varphi \to 0$), then the maximum possible work ($W_{max}$) done by $F_z$ is given by eq (8).

$$\begin{aligned} W_{max} &= \int F_z \mathrm{d}L \\ &= \int P\pi r R^2 \sin^2\theta \mathrm{d}L \\ &= \int P\pi R^2 \sin^2\theta R\sin\theta \mathrm{d}\theta \\ &= \int P\pi R^3 \sin^3\theta \mathrm{d}\theta \\ &= P\pi R^3\left(\frac{1}{3}\cos^3\varphi - \cos\varphi + \frac{2}{3}\right) \end{aligned} \tag{8}$$

where d$L$ is the differential vertical $z$ displacement.

We can now compare $W_{max}$, $\alpha E_{binding}$, and $E_{k,max}$. For calculation purposes, we consider the nAl/NC mesoparticle with $\varphi = 10°$, i.e., partially embedded in HTPB. The results of this calculation are shown in Figure 9. The reader is reminded

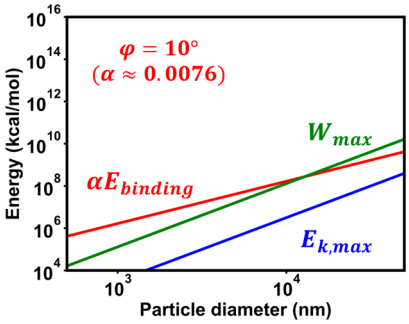


**Figure 9.** Dependency of $W_{max}$, $\alpha E_{binding}$, and $E_{k,max}$ on particle diameter when $\varphi = 10°$ ($\alpha \approx 0.0076$).

that the $x$-axis is the diameter of the mesoparticle, which is composed of Al nanoparticles and NC as the binder. The work done by the gas expansion is much larger than $E_{k,max}$, suggesting that the role of the dragging of the gaseous HTPB pyrolysis product is neglectable compared to the gas expansion from NC. Meanwhile, $W_{max}$ is comparable to or even higher than $\alpha E_{binding}$, suggesting that assembling nAl and NC into a mesoparticle is a feasible strategy to lift nAl embedded in HTPB.

## 4. CONCLUSIONS

Molecular dynamics simulation of Al-core-$Al_2O_3$-shell particles within HPTB is explored to explain the experimental observation that in stagnation-flow burners containing metalized polymer fuel, micrometer-sized Al particles will eject from the surface while nanometer-sized Al particles will not.

Comparing the polymer−particle interaction energy with the maximum kinetic energy imparted to particles from the lifting force during polymer pyrolysis, we find that nanosized Al is difficult to eject from the surface due to its increased polymer−particle interaction binding energy, while microsized Al is easier. To solve this issue, we propose a strategy that replaces Al nanoparticles with nAl/NC mesoparticles. Theoretical analysis indicates that the gas expansion from NC decomposition can generate sufficient kinetic energy to overcome the binding energy with the polymer, much more effective than the dragging of the HTPB pyrolysis product.

## AUTHOR INFORMATION

### Corresponding Author

**Michael R Zachariah** − *Department of Chemical and Environmental Engineering, University of California, Riverside, California 92521, United States;* orcid.org/0000-0002-4115-3324; Email: mrz@engr.ucr.edu

### Author

**Yuxin Zhou** − *Department of Chemical and Environmental Engineering, University of California, Riverside, California 92521, United States;* orcid.org/0009-0005-1397-3834

Complete contact information is available at: https://pubs.acs.org/10.1021/acs.jpcc.4c08542

### Notes

The authors declare no competing financial interest.

## ACKNOWLEDGMENTS

This work is supported by an ONR-MURI.

## REFERENCES

(1) Hastings, D. L.; Schoenitz, M.; Dreizin, E. L. High Density Reactive Composite Powders. *J. Alloys Compd.* **2018**, *735*, 1863−1870.

(2) He, W.; Liu, P.-J.; He, G.-Q.; Gozin, M.; Yan, Q.-L. Highly Reactive Metastable Intermixed Composites (MICs): Preparation and Characterization. *Adv. Mater.* **2018**, *30* (41), No. 1706293.

(3) Dreizin, E. L. Metal-Based Reactive Nanomaterials. *Prog. Energy Combust. Sci.* **2009**, *35* (2), 141−167.

(4) Mazloomi, K.; Gomes, C. Hydrogen as an Energy Carrier: Prospects and Challenges. *Renewable and Sustainable Energy Reviews* **2012**, *16* (5), 3024−3033.

(5) Sinha, Y. K.; Sridhar, B. T. N.; Kishnakumar, R. Study of Thermo-Mechanical Properties of HTPB−Paraffin Solid Fuel. *Arab J. Sci. Eng.* **2016**, *41* (11), 4683−4690.

(6) Quagliano Amado, J. C.; Ross, P. G.; Mattos Silva Murakami, L.; Narciso Dutra, J. C. Properties of Hydroxyl-Terminal Polybutadiene (HTPB) and Its Use as a Liner and Binder for Composite Propellants: A Review of Recent Advances. *Propellants, Explosives, Pyrotechnics* **2022**, *47* (5), No. e202100283.

(7) Dennis, C.; Bojko, B. On the Combustion of Heterogeneous AP/HTPB Composite Propellants: A Review. *Fuel* **2019**, *254*, No. 115646.

(8) Geipel, C. M.; Bojko, B. T.; Pfützner, C. J.; Fisher, B. T.; Johnson, R. F. Regression of Solid Polymer Fuel Strands in Opposed-



https://doi.org/10.1021/acs.jpcc.4c08542
J. Phys. Chem. C 2025, 129, 5696−5701

Flow Combustion with Gaseous Oxidizer. *Proceedings of the Combustion Institute* **2023**, *39* (3), 3389−3399.
(9) Eckart, S.; Yu, C.; Maas, U.; Krause, H. Experimental and Numerical Investigations on Extinction Strain Rates in Non-Premixed Counterflow Methane and Propane Flames in an Oxygen Reduced Environment. *Fuel* **2021**, *298*, No. 120781.
(10) Cuoci, A.; Frassoldati, A.; Faravelli, T.; Ranzi, E. Extinction of Laminar, Premixed, Counter-Flow Methane/Air Flames under Unsteady Conditions: Effect of H2 Addition. *Chem. Eng. Sci.* **2013**, *93*, 266−276.
(11) Parr, T. P.; Hanson-Parr, D. M.; Smooke, M. D.; Yetter, R. A. AP/(N2+C2H2+C2H4) Gaseous Fuel Diffusion Flame Studies. *Proceedings of the Combustion Institute* **2005**, *30* (2), 2113−2121.
(12) Fuse, R.; Kobayashi, H.; Ju, Y.; Maruta, K.; Niioka, T. NOx Emission from High-Temperature Air/Methane Counterflow Diffusion Flame. *International Journal of Thermal Sciences* **2002**, *41* (7), 693−698.
(13) Young, G.; Risha, G.; Miller, A. G.; Glass, R. A.; Connell, T. L. Jr.; Yetter, R. A. Combustion of alane-based solid fuels. *Int. J. Energ. Mater. Chem. Propul.* **2010**, *9* (3), 249.
(14) Yuan, X.; Zhang, S.; Gou, R.; Huang, Y.; Bai, H.; Guo, Q. ReaxFF/Lg Molecular Dynamics Study on Thermolysis Mechanism of NTO/HTPB Plastic Bonded Explosive. *Computational and Theoretical Chemistry* **2022**, *1215*, No. 113834.
(15) Feng, M.; Li, H.; Luo, K. H. A Molecular Dynamics Study on Oxidation of Aluminum Hydride (AlH3)/Hydroxyl-Terminated Polybutadiene (HTPB) Solid Fuel. *Proceedings of the Combustion Institute* **2021**, *38* (3), 4469−4476.
(16) Zhou, Y.; Zachariah, M. R. Molecular Dynamics Study on the Capture of Aluminum Particles by Carbon Fibers during the Propagation of Aluminum-Based Energetics. *Energy Fuels* **2024**, *38* (10), 8992−9000.
(17) Hong, S.; van Duin, A. C. T. Atomistic-Scale Analysis of Carbon Coating and Its Effect on the Oxidation of Aluminum Nanoparticles by ReaxFF-Molecular Dynamics Simulations. *J. Phys. Chem. C* **2016**, *120* (17), 9464−9474.
(18) Cheng, Y.-X.; Zhao, Y.; Zhao, F.-Q.; Xu, S.-Y.; Ju, X.-H.; Ye, C.-C. ReaxFF Simulations on the Combustion of Al and *n*-Butanol Nanofluid. *Fuel* **2022**, *330*, No. 125465.
(19) Thompson, A. P.; Aktulga, H. M.; Berger, R.; Bolintineanu, D. S.; Brown, W. M.; Crozier, P. S.; in't Veld, P. J.; Kohlmeyer, A.; Moore, S. G.; Nguyen, T. D.; et al. LAMMPS - a Flexible Simulation Tool for Particle-Based Materials Modeling at the Atomic, Meso, and Continuum Scales. *Comput. Phys. Commun.* **2022**, *271*, No. 108171.
(20) Evans, D. J.; Holian, B. L. The Nose−Hoover Thermostat. *J. Chem. Phys.* **1985**, *83* (8), 4069−4074.
(21) Chowdhury, M.; Ghildiyal, P.; Rojas, A.; Wang, Y.; Wang, H.; Zachariah, M. R. High-Yield Spray Drying Assembly and Reactive Properties of Nanoenergetic Mesoparticle Composites. *Advanced Powder Technology* **2023**, *34* (7), No. 104075.
(22) Wang, Y.; Chowdhury, M.; Zhou, Y.; Issac Paul, G.; Shi, K.; Zachariah, M. R. Oscillating-to-Continuous Combustion Transition in Mesoparticle Composites Through Manipulation of Heat Feedback. *Adv. Funct. Mater.* **2024**, *34* (42), No. 2406722.
(23) Jacob, R. J.; Wei, B.; Zachariah, M. R. Quantifying the Enhanced Combustion Characteristics of Electrospray Assembled Aluminum Mesoparticles. *Combust. Flame* **2016**, *167*, 472−480.
(24) Young, G.; Wang, H.; Zachariah, M. R. Application of Nano-Aluminum/Nitrocellulose Mesoparticles in Composite Solid Rocket Propellants. *Propellants, Explosives, Pyrotechnics* **2015**, *40* (3), 413−418.
(25) Zhou, L.; Piekiel, N.; Chowdhury, S.; Zachariah, M. R. T-Jump/Time-of-Flight Mass Spectrometry for Time-Resolved Analysis of Energetic Materials. *Rapid Commun. Mass Spectrom.* **2009**, *23* (1), 194−202.
(26) Zhou, Y.; Shi, K.; Chowdhury, M.; Hagen, E.; Wang, Y.; Zachariah, M. R. Direct Microscopic Imaging of Exploding Aluminum/Nitrocellulose Mesoparticles to Reveal the Enhanced Combustion Mechanism. *Fuel* **2025**, *387*, No. 134348.





https://doi.org/10.1021/acs.jpcc.4c08542
J. Phys. Chem. C 2025, 129, 5696−5701